Quaternary Research **57**, 9–21 (2002)
doi:10.1006/qres.2001.2284, available online at http://www.idealibrary.com on IDEAL®

Lake Levels and Sequence Stratigraphy of Lake Lisan, the Late Pleistocene Precursor of the Dead Sea

Yuval Bartov,[1] Mordechai Stein, Yehouda Enzel, Amotz Agnon, and Ze'ev Reches

The Institute of Earth Sciences, The Hebrew University of Jerusalem, Givat Ram 91904, Israel

Received October 18, 2000

Lake Lisan, the late Pleistocene precursor of the Dead Sea, existed from ~70,000 to 15,000 yr B.P. It evolved through frequent water-level fluctuations, which reflected the regional hydrological and climatic conditions. We determined the water level of the lake for the time interval ~55,000–15,000 cal yr B.P. by mapping offshore, nearshore, and fan-delta sediments; by application of sequence stratigraphy methods; and by dating with radiocarbon and U-series methods. During the studied time interval the lake-level fluctuated between ~340 and 160 m below mean sea level (msl). Between 55,000 and 30,000 cal yr B.P. the lake evolved through short-term fluctuations around 280–290 m below msl, punctuated (at 48,000–43,000 cal yr B.P.) by a drop event to at least 340 m below msl. At ~27,000 cal yr B.P. the lake began to rise sharply, reaching its maximum elevation of about 164 m below msl between 26,000 and 23,000 cal yr B.P., then it began dropping and reached 300 m below msl at ~15,000 cal yr B.P. During the Holocene the lake, corresponding to the present Dead Sea, stabilized at ca. 400 m below msl with minor fluctuations. The hypsometric curve of the basin indicates that large changes in lake area are expected at above 403 and 385 m below msl. At these elevations the lake level is buffered. Lake Lisan was always higher than 380 m below msl, indicating a significantly large water contribution to the basin. The long and repetitious periods of stabilization at 280–290 m below msl during Lake Lisan time indicate hydrological control combined with the existence of a physical sill at this elevation. Crossing this sill could not have been achieved without a dramatic increase in the total water input to the lake, as occurred during the fast and intense lake rise from ~280 to 160 m below msl at ~27,000 cal yr B.P. © 2002 University of Washington.

Key Words: **Dead Sea; Lake Lisan; late Pleistocene; lake levels; paleoclimatology; lacustrine deposits; fan-delta; sequence stratigraphy.**

INTRODUCTION

Lake Lisan, the late Pleistocene precursor of the Dead Sea, existed from ~70,000 to 15,000 yr B.P. (Kaufman, 1971; Kaufman *et al.*, 1992; Schramm, 1997; Schramm *et al.*, 2000). It occupied the tectonic depression along the Dead Sea basin and the Jordan Valley (Fig. 1). The Dead Sea basin is located between steep margins in the east and west and flat shoulders to the south and north that are bordered by topographical sills. This basin configuration and the hydrological history of the drainage area control the pattern of lake-level changes. The steep margins of the basin recorded small lake-level changes, while the flat margins were sensitive mainly to major hydrological changes. The ability to determine shoreline elevations and to date them enabled the construction of a lake-level curve. This curve serves as a tool for evaluating hydrologic changes and regional climate events during the last glacial period.

In this study, we determined the lake-level curve of Lake Lisan for the time interval ~55,000 to 15,000 cal yr B.P. The curve is based on the recognition and dating of shoreline deposits in the well-preserved fan sequence of the Ze'elim delta in the Massada plain (Fig. 1). The Massada plain is located in the central part of the Dead Sea basin south of the Ze'elim valley, on the downthrown side of the western border faults of the basin (Fig. 1). The study area was chosen for the following reasons: 1) The deeply incised wadis in this area display excellent exposures of the Lisan Formation. 2) A variety of depositional environments were recognized in the area (Neev and Emery, 1967; Begin *et al.*, 1974; Sneh, 1979; Manspeizer, 1985; Frostick and Reid, 1989), and they can be correlated physically and stratigraphically. 3) The stratigraphic sections correlate well with the stratigraphic sections of the Perazim valley that were dated by Schramm *et al.* (2000) and analyzed by Machlus *et al.* (2000). 4) The location chosen provides critical and complementary features: high-energy clastic sediments of the stream, delta, and shore environments that interfinger with low-energy lake sediments. This combination frequently preserved the shoreline deposits and provides a rare opportunity for physical correlation of shore and offshore units. As the deposits of Lake Lisan contain dateable aragonite laminae (Kaufman, 1971; Schramm *et al.*, 2000), this correlation provides accurate dating of the observed shoreline deposits.

In this study, we apply facies analysis to the well-preserved fan sequence of the Ze'elim delta, we construct a lake-level curve, and, finally, we discuss the basin hypsometry, as well as its relation to the lake-level and climate.

[1] To whom correspondence should be addressed. E-mail: yuval@vms.huji.ac.il.

0033-5894/02 $35.00
Copyright © 2002 by the University of Washington.
All rights of reproduction in any form reserved.

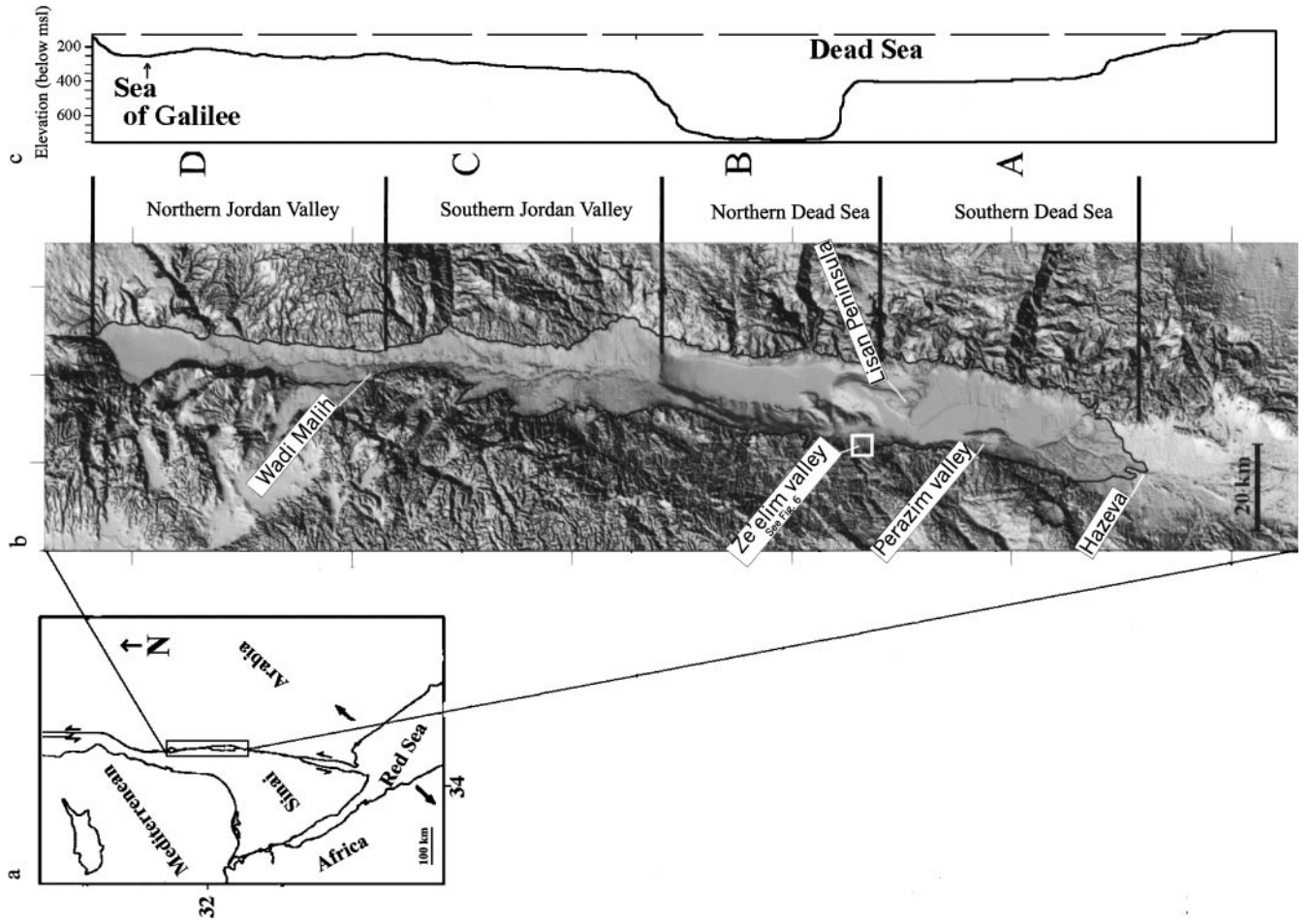

FIG. 1. (a) Location map of the study area. (b) Shaded relief map of the Dead Sea basin–Jordan Valley. The dark line marks the extent of Lake Lisan at 164 m below msl. (c) Present-day north–south topographic section along the Dead Sea basin–Jordan Valley, with four subbasins (Basins A to D) and the proposed high stand at 164 m below msl.

STRATIGRAPHIC ANALYSIS

Late Pleistocene Sediments in the Massada Plain

The exposed late Pleistocene sediments in the Massada plain comprise the Samra Formation and the overlying Lisan Formation (Fig. 2). The uppermost part of Samra Formation consists of interlayered aragonite lamina, and carbonate sand and silt. The Lisan Formation was deposited in two environments: (a) an offshore environment with alternating aragonite and detrital laminae consisting mainly of silt-sized calcite, dolomite, and quartz; and (b) a shore–delta environment with clastic sediments, which consist of sand, pebbles, and boulders.

The Lisan Formation is divided here into three members, which are bound in offshore sections by prominent gypsum layers that were traced laterally over a large distance basinwards (Fig. 2). The Lower and Upper members in the offshore sections consist mainly of alternating laminae of aragonite and silt-sized clasts, while the Middle Member contains large portions of sandy layers. This stratigraphic division follows the one that was established in the PZ1 section of the Perazim valley (Machlus *et al.*, 2000). The lithology reflects the lake-level conditions, which generally fluctuated between high stands (Upper and Lower members) and a relatively lower stand during the Middle Member.

Stratigraphic Correlation between the Massada Plain and the Perazim Valley

The Perazim valley sections (PZ1; PZ2 of Machlus *et al.*, 2000) are located about 20 km south of the Massada plain. The difference in elevation between the two sites is ∼70 m (Fig. 2). The correlation between the two sections is based on radiometric dating and the identification of several stratigraphic markers, such as the three prominent gypsum layers found at the bottom of the sections and the identification of unconformities within the exposed sections.

The Upper Member of the Lisan Formation exhibits similar thickness in both sections and is composed of alternating aragonite and silt laminae with prominent gypsum layers at the top. The aragonite laminae sampled beneath the upper gypsum in both sections yielded an age of ∼19,000 cal yr B.P., and the

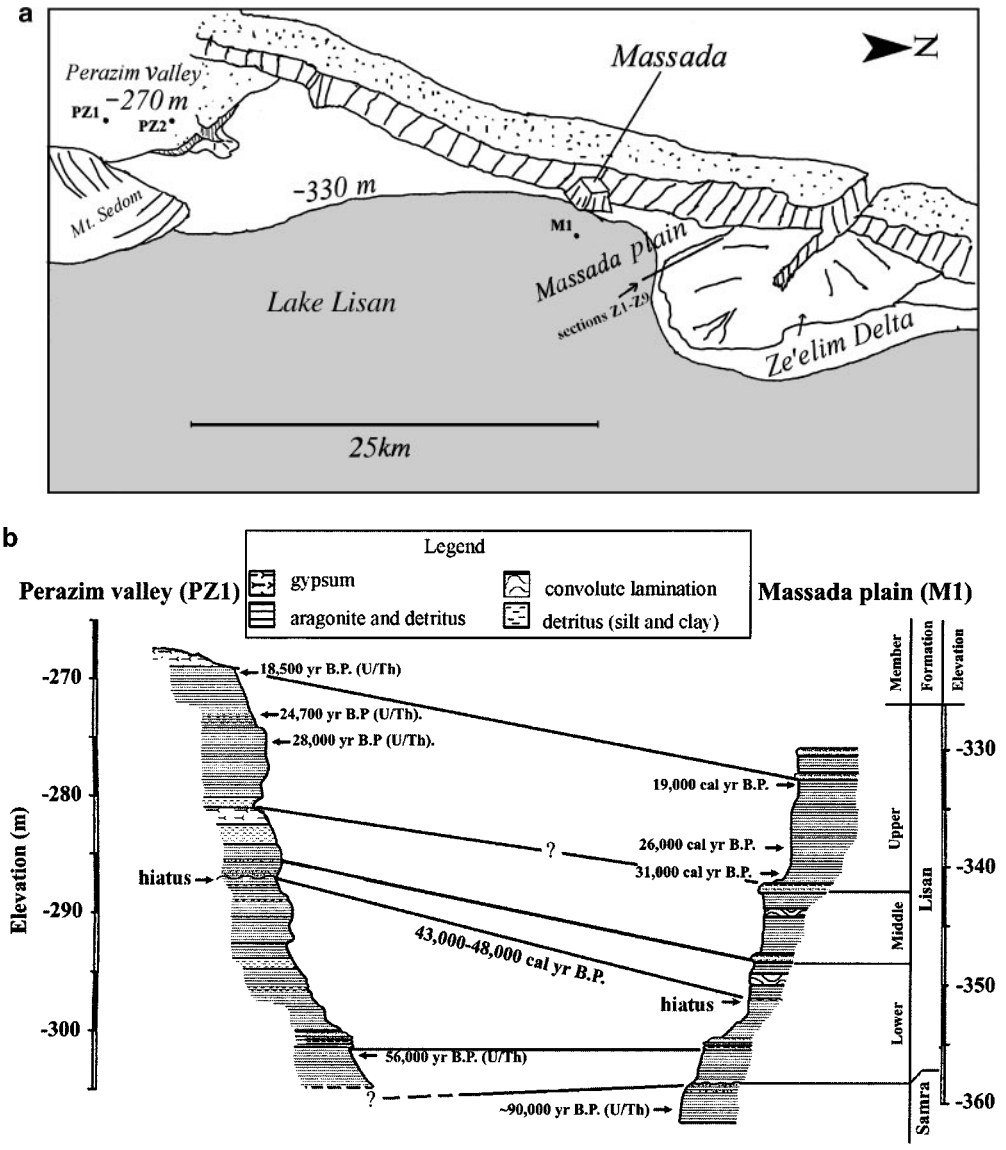

FIG. 2. (a) A paleogeographic reconstruction of the Massada plain and the Perazim valley at ~46,000 cal yr B.P. when the lake level was at 330 m below msl. A large part of the Massada plain was under water, while the Perazim valley was subjected to subaerial erosion and stream incision. (b) Correlation between the sections of the Lisan Formation in the Massada plain and the Perazim valley, based on stratigraphic markers (e.g., the three gypsum layers in the Lower Member of the formation) and U-series and radiocarbon ages (Schramm *et al.*, 2000, and Table 2).

aragonite at the bottom of the Upper Member yielded an age of ~31,000 cal yr B.P.

The elevation difference between the Massada and the Perazim sections reflects the original morphology of the basin, since the syn- and post-Lisan Formation tectonic movements are on the order of only a few meters (Marco and Agnon, 1995). Large post-Lisan tectonic displacements of about 7 m were observed only at the western margin of the Massada plain close to the mountain front (Fig. 3) (Bartov, 1999). The estimated tectonic movement in the Perazim valley is about 2 m (Marco *et al.*, 1996). Thus, we assume that the tectonic movements played a minor role and account for less than 10 m of the 70-m elevation difference, with the rest being pre-Lisan Formation relief. Therefore, when the water level dropped and a beach environment dominated the Perazim valley, gypsum or aragonite laminae were deposited on the Massada plain at a depth of a few tens of meters. The reconstruction of the lake level is based on data from different locations in the basin, assuming that elevation reflects time. For example, the Massada plain (M1 section, Fig. 2) was under water, while the higher Perazim valley was already exposed; thus the two locations provide complementary information on the location of the shorelines over time.

Sedimentary Environments

We used the depositional environments of the present-day Dead Sea as a model for the fan-delta, shore deposits, and

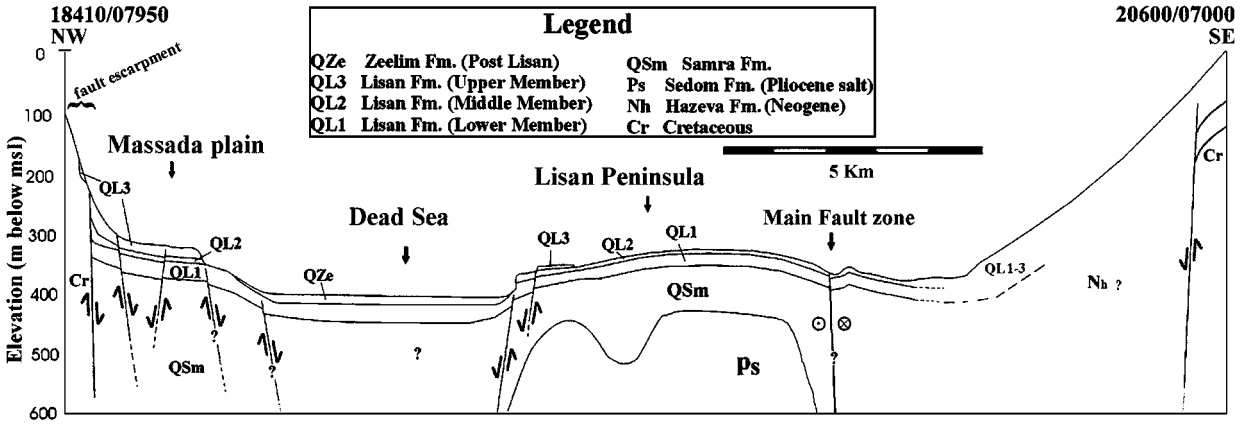

FIG. 3. Geological cross section between the Massada plain and the Lisan Peninsula (see Fig. 1) presenting the Lisan Formation sediments (QL1–3) in different morphological settings of the Dead Sea basin such as the basin border escarpment and a flat plain (e.g., the Massada plain). The Lisan Formation in the Lisan Peninsula is uplifited by the Pliocene salt diapir of the Sedom Formation. The main fault of the Dead Sea Transform is located to the east of the Lisan Peninsula (Garfunkel, 1981; Bartov, 1999).

offshore environments of Lake Lisan. The present-day Dead Sea developed over approximately the past 3000 yr (Klein, 1984; Bowman, 1997; Kadan, 1997; Ben-David, 1998; Enzel *et al.*, 2000; Ken-Tor *et al.*, 2001). At present (year 2001), the water level is 414 m below mean sea level (msl), significantly lower than the Lake Lisan level, which fluctuated between ∼160 m (Bowman and Gross, 1992) and 340 m below msl (Bartov, 1999). Nevertheless, on the basis of geomorphic and geochemical considerations, we think that the environments of deposition and their relative distribution in Lake Lisan were similar to those of the Dead Sea. The sedimentary conditions were particularly similar during low stands. Moreover, some components of the sedimentary facies of the Lisan Formation are observed in the present-day Dead Sea (e.g., beach ridges). The following environments were recognized in both lakes.

Alluvial environment. Alluvial fan sediments dominate the margins of the study area (Fig. 2a). Most of the fans are braided channels with debris-flow deposits (Table 1 and Fig. 4a), mainly composed of Upper Cretaceous cobbles and pebbles. The alluvial fans are characterized by planar cross-stratified sand and ripple cross-lamination at their distal parts, whereas coarser deposits dominate their proximal portions.

Beach environment. Beach ridges are composed of platy pebbly clinoforms dipping 5° to 30° lakeward (foresets, Bc1 in Fig. 5, Table 1) and shoreward (backset, Bc2) (after Renaut and Owen, 1991; Blair, 1999). Silty thin beds (∼2 cm thick) overlain by sand and unsorted pebbles are interpreted to be lagoon deposits at the back of the ridge (Bc3 in Fig. 5, Table 1) (Kadan, 1997; Adams and Wesnousky, 1998; Enzel *et al.*, 2000). In outcrops of the Lisan Formation the beach ridges overlie either shallow water deposits, such as rippled sands, or deeper lake sediments. This stratigraphic relationship implies rapid small-scale changes in lake level. Behind the ridges, wash-over silt deposits accumulated in small lagoons that were filled by sediments of fluvial origin during the recessional stage of the same flood or by a later one.

Beach ridges of the present-day Dead Sea are commonly associated with large storms, usually after floods transport large amounts of coarse alluvial sediment into the lake, depositing them at the mouths of the streams (Kadan, 1997). These sediments are then sorted by waves and washed back to the beach during storms. In some cases, as a result of intensive wave action, the larger pebbles are deposited on top of the beach ridge. Thus, beach and lagoon deposits clearly mark paleolake levels and are preserved mostly on low-angle slopes (Adams and Wesnousky, 1998; Oviatt, 2000).

Delta environment. In general the delta environment displays clastic sediments that become finer and better sorted toward the lake (from large boulders to fine sand and silt) and are restricted to the outlets of the rivers entering the lake (Nemec and Steel, 1988). In Lake Lisan, changes of lake level and sediment supply control the delta buildup. When the lake level rises, sediments of deeper water (aragonite and silt) cover the fan with occasional coarser grain deposits entering from the basin margins (NS1 in Fig. 5, Table 1). When the lake level drops, the delta front is built of foresets (NS2), with either thin topset accumulation (indicating sedimentary bypass) or truncation and channeling at the proximal part of the delta. These processes generate an interfingering relationship between the lake and the near-shore environments.

Offshore environment. The offshore deposits of Lake Lisan consist mostly of laminated aragonite and silt-sized detrital carbonate, quartz, and clay (DL3, 4 in Fig. 5, Table 1). Halite and gypsum sometimes form laminae or thin beds. The aragonite precipitated from the upper layer of a stratified lake and required an input of freshwater containing bicarbonate (Stein *et al.*, 1997), whereas the clastic material derived from the basin shoulders. The clastic material includes dolomite, calcite, clay,

TABLE 1
Facies and Environment Interpretation for the Lisan Formation

Facies symbol	Facies description	Depositional environment	Estimated water depth	Examples for general reference and for the Dead Sea
AL1	Large poorlysorted, carbonate boulders	Debris talus along the basin margin	Above water level	Nemec and Steel, 1984
AL2	Poorlysorted subparallel-stratified to nonstratified pebbles to cobbles of carbonate or chert (rare), with coarse sand to silt as matrix	Braided stream or debris flow	Above water level	Nemec and Steel, 1984; Frostrick and Reid, 1989; Ben-David, 1998
AL3	Medium sorted sand to pebbles, planar cross-stratified sets, sometimes with fine-bedded cross-laminated sand	Braided stream at distal portion of alluvial fan	Above water level	Frostick and Reid, 1989
Bc1	Very well-sorted platy pebbly clinoforms dipping 5°–30° facing lakeward (foresets), either sand supported or grain supported	Beach ridge	0–1 m	Renaut and Owen, 1991; Blair, 1999; Kadan, 1997
Bc2	Very well-sorted platy pebbly clinoforms dipping 10°–50° facing landward (backsets) sand supported	Beach ridge	0 m (always deposited above water level)	Renaut and Owen, 1991; Blair, 1999; Kadan, 1997
Bc3	Finely laminated to bedded silt and sand with a total thickness of 10–20 cm	Lagoon	0 m (always deposited above or at water level)	Kadan, 1997; Adams and Wesnousky, 1998
NS1	Medium to fine well-sorted sand cross-bedded sets, laminations dipping 5°–25°; occasional pebbles, symmetric ripple marks and pebbly lobes	Nearshore wave influenced	1–5 m	Sneh, 1979; Ethridge and Wescott, 1984; Machlus *et al.*, 2000
NS2	Very fine sand to silt, well-sorted dipping 5°–10°; occasional coarse sand lobes	Nearshore below-wave influence	Estimated 1–15 m	Sneh, 1979; Ethridge and Wescott, 1984; Machlus *et al.*, 2000
L1	Well-sorted pebbles with occasional cobbles dipping lakeward 20°–50°	Prograding delta	Estimated 2–10 m	Bartov, 1999
L2	Well-sorted sand to granules in gently inclined cross beds; occasional climbing ripples	Delta front	Estimated 10–20 m	Bartov, 1999
L3	Pebbles to silt layers or lenses overlain and underlain by laminae of DL facies	Interfingering delta–lacustrine	Estimated 10–20 m	Bartov, 1999
DL1	Massive grayish to brownish silt beds may contain gypsum or halite layers	Lacustrine	Variable	Bartov, 1999
DL2	Finely laminated 0.1–2 mm alternating aragonite and detritus (silt, clay calcite, and quartz)	Lacustrine	Variable	Begin *et al.*, 1974

quartz, and very fine-grained rock fragments (Begin *et al.*, 1974) derived from the Cretaceous bedrock of the Lisan drainage basin. The quartz grains could be of aeolian origin (Stein, 2000).

Sequence Stratigraphy Synthesis of Lake Lisan Deposits

The establishment of a lake-level history can be approached in two ways. The sequence architecture of the sedimentary record can be analyzed in terms of stratigraphic sequences that contain information on transgressions and regressions of the lake, and certain types of sediments, e.g., beach deposits, can define the shoreline locations. Here, we apply the two approaches to examine Lake Lisan sediments and reconstruct a lake-level curve.

Following the scheme of Posamentier *et al.* (1992), we find that the sequence architecture of the Lisan Formation can be attributed to three factors: base-level (in this case, lake-level) changes, morphology, and the geographical location of sediment input to the basin. The shore position defines the lake-level curve, but for constructing a smoother curve, knowledge of the water depth between two beach deposits in a cycle is necessary. The relatively wide and flat topography of the lake margins in the Massada plain preserved most of the sedimentary sequences, enabling estimation of the approximate water depth for the observed facies (Bartov, 1999; Machlus *et al.*, 2000; Oviatt, 2000). Under these conditions, limits could be placed on the lake level between data points representing beach lines on the curve. Another important factor in establishing a lake-level curve is to have a system with low-energy sediment input. This condition is required to reduce truncation and could produce a systems tract that can be traced laterally. At the sides of the fan-deltas, low erosion rates exist, especially at low lake levels, when parts of the delta are exposed and the sedimentary input bypasses through rejuvenated channels.

Figure 5 illustrates schematic concepts for the sedimentary sequence generated in an area of flat topography (e.g., Massada plain) during lake-level fluctuations. Figure 5a illustrates the

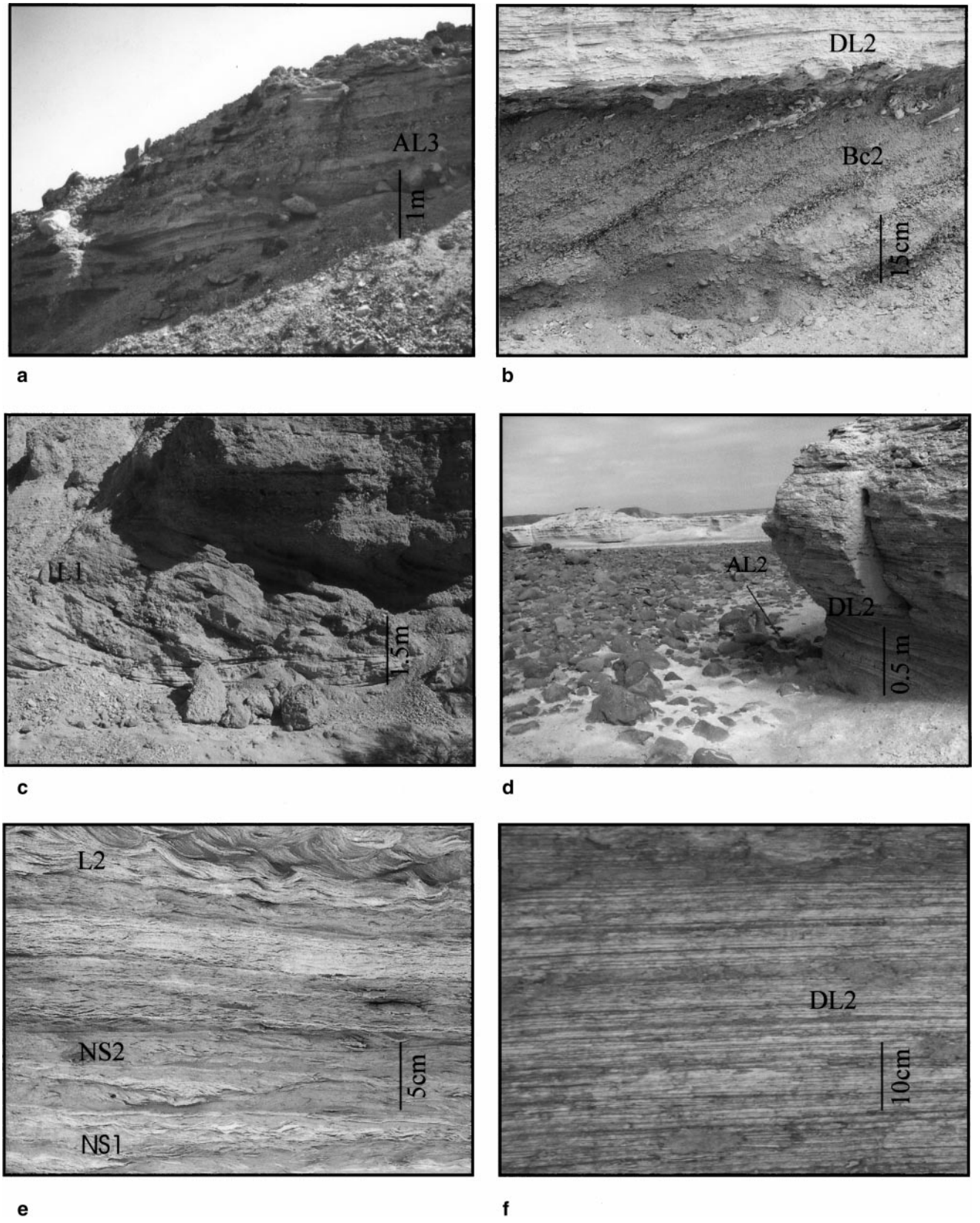

FIG. 4. Photographs from sections Z1–Z11 in the Massada plain, illustrating the different facies of the Lisan Formation. (a) Debris flow and braided stream deposits of the alluvial fan complex (AL3, section Z9). (b) Beach ridge of pebbles and sand facing shoreward (backset, Bc2 in section Z2) topped by aragonite crusts, laminated aragonite, and silty laminae (DL2). (c) Fan-delta sets (L1); note the topsets, foresets, and bottom sets (section Z9). (d) Alluvial fan surface (AL2) topped by deeper lake sediments (DL2) from the upper part of the Lower Member of the Lisan Formation. (e) Symmetric ripples and sand lobes (N1, NS2) topped by climbing ripples of deeper environment (L2, section Z2). (f) Alternating aragonite (light) and silt laminae (dark) (DL2, section M1).

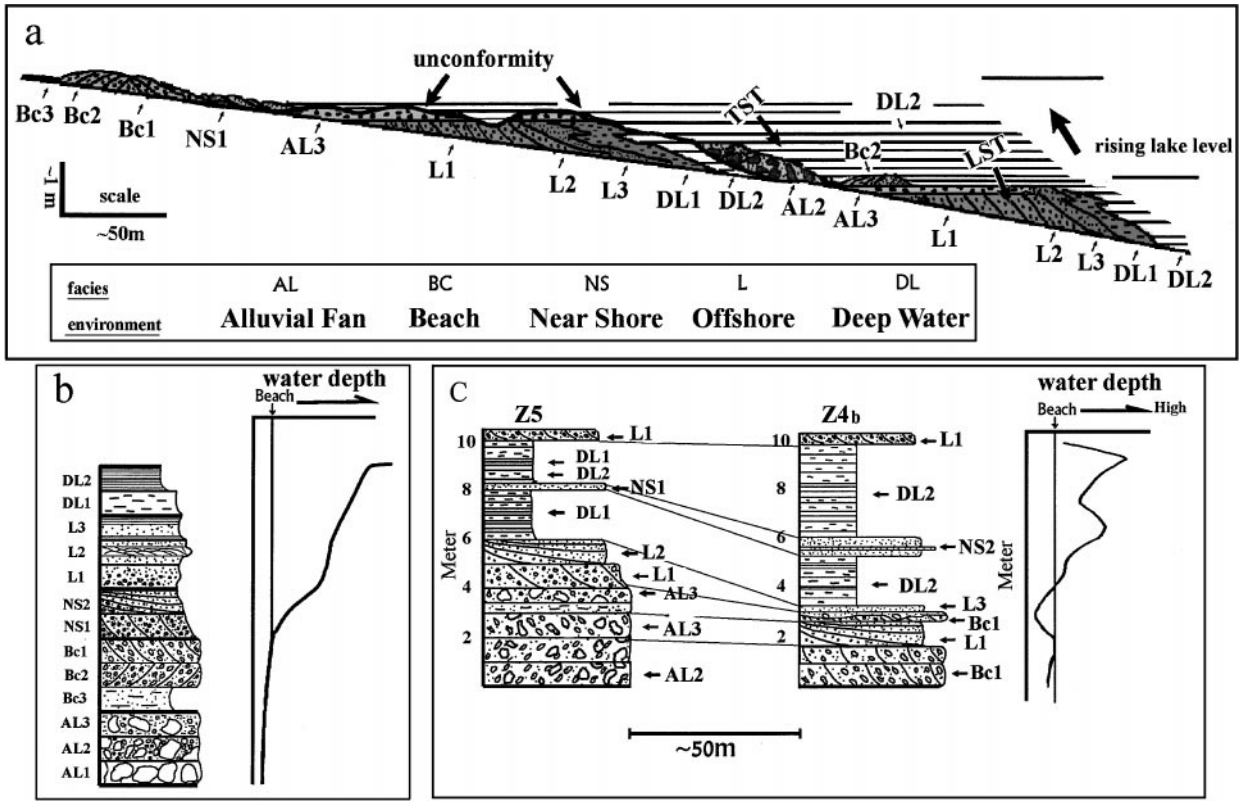

FIG. 5. Facies distribution on the flat topography area of the Massada plain. (a) Schematic cross section of the depositional systems' response to a fluctuating lake level. Note the forced regressive architecture of the low-stand systems tract (LST) and the transgressive systems tract (TST) with beach deposits at the left end overlying an unconformity. (b) Schematic fining-upward sequence and a water-depth curve reflecting a landward shift of facies due to a rise in lake level. This is a full sequence from subaerial (AL) to deep lake (DL) environments nearby or at the edge of a fan-delta (for details see text and Table 1). (c) Correlation between two measured profiles in the Massada plain (sections Z5 and Z4).

horizontal distribution of facies from the subaerial environment (AL) to deep lake (DL) offshore deposits, generating a fining-upward sequence during a landward shift in the beach position. The full cycle is shown schematically in Figure 5b. Subaerial alluvial sediment, beach deposits, or a laterally traced unconformity mark the base of the cycle (facies AL and Bc). Up-sequence, cross-bedded delta deposits show a fining-upward sequence that interfingers with offshore deposits, silts, and evaporites of aragonite and occasional gypsum layers. In areas of flat topography away from the basin borders, facies recognition is a good proxy for lake-level oscillations (Fig. 5c, Table 1).

The cyclic stratigraphy of the Lisan Formation in the Massada plain is presented by a 2-km-long profile with 10 measured stratigraphic sections along the southern distal portion and toe of the Ze'elim delta (Fig. 6). The correlation between the sections is based on marker beds that were physically traced in the field from offshore to nearshore environments. The elevations and distances of the sections were measured by using an electronic distance measurement (EDM) total station. The chronological framework for the analysis presented is based on several ^{14}C and ^{234}U-^{230}Th ages (Table 2) that were obtained from aragonite laminae in the sections in the Massada plain and from the stratigraphic correlation with the high-resolution dated section of the Perazim valley.

Two main sequences defined by major unconformities were identified in the exposures of the uppermost part of the Samra Formation and the Lisan Formation in the study area. Here we focus on the description of the upper sequence (within the Lisan Formation) that extends from the sedimentary hiatus at ~48,000 to 43,000 cal yr B.P. (Fig. 2b) to the top Lisan Formation (at ~15,000 cal yr B.P.). The lower sequence contains one stratigraphic cycle (designated as cycle I in Fig. 6) from the Lisan Formation, and the upper sequence is composed of five high-order stratigraphic cycles (designated as cycles II–VI). The stratigraphic analysis of the different cycles was carried out by correlating several sections in the Massada plain. The sections display an overall change from an offshore depositional environment in the east to a nearshore–onshore depositional environment in the west. Section M1, which is located 3 km to the south of the other sections in the Ze'elim delta (Z1-Z9, Fig. 6), represents a deeper lake environment. It is correlated with section Z1 by using distinctive gypsum layers. Sections Z2 to Z9 are correlated by cycle boundaries and marker beds. Following is a description of the cycle analyses.

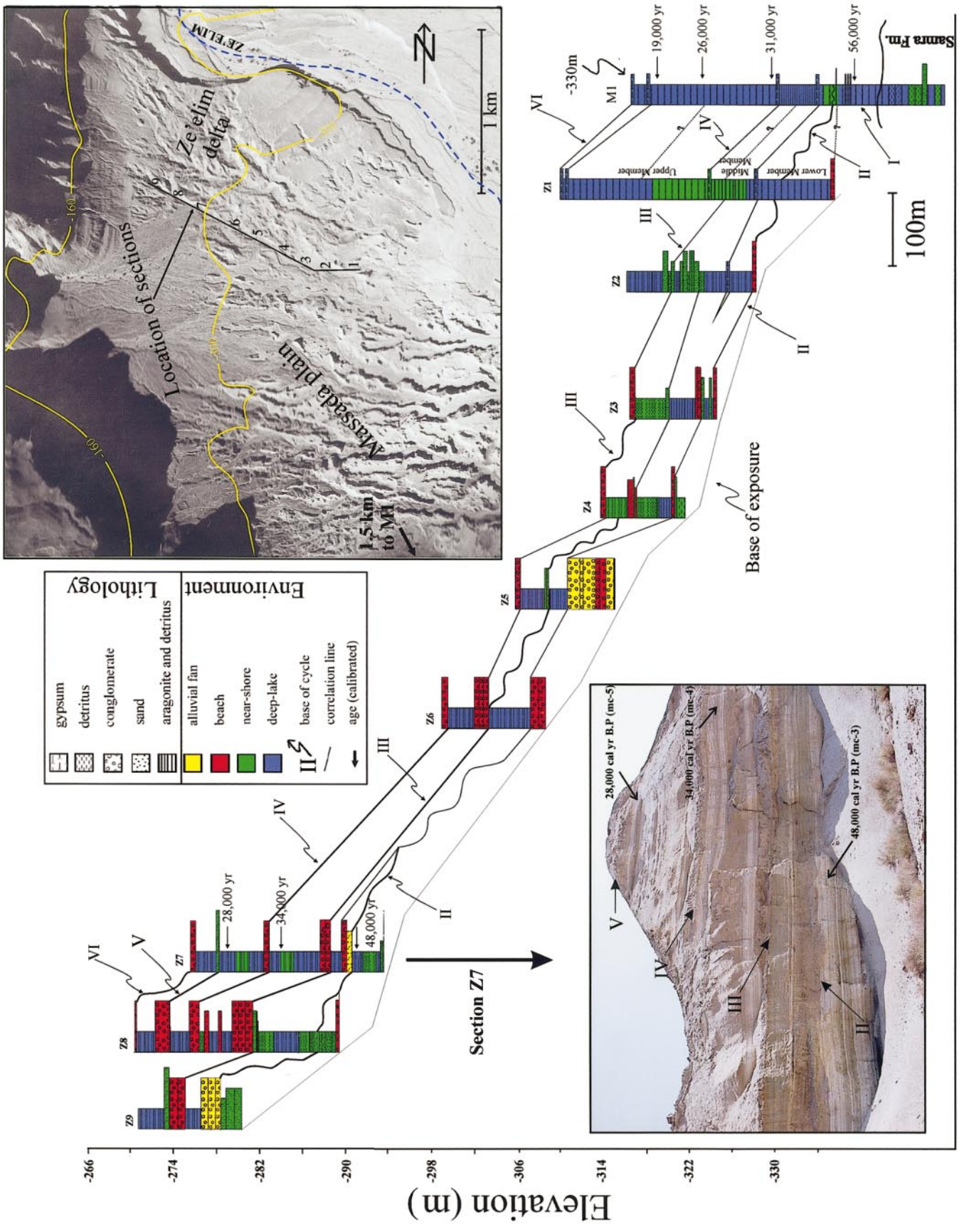
Location of sections
Ze'elim delta
Massada plain
1.5 km to M1
1 km
Environment
alluvial fan
beach
near-shore
deep-lake
base of cycle
correlation line
age (calibrated)
Lithology
gypsum
detritus
conglomerate
sand
aragonite and detritus
Section Z7
Base of exposure
Elevation (m)
-266
-274
-282
-290
-298
-306
-314
-322
-330
28,000 cal yr B.P (mc-5)
34,000 cal yr B.P (mc-4)
48,000 cal yr B.P (mc-3)
Lower Member
Middle Member
Upper Member
Samra Fm.
19,000 yr
26,000 yr
31,000 yr
56,000 yr
-330m
100m

TABLE 2
Radiocarbon Ages of Separated Millimeter-Scale Aragonite Laminae and Their Absolute Elevations in the Sections (See Fig. 6)

Sample	Location[a]	Elevation (m below msl)	Radiocarbon age (^{14}C yr B.P.)[b]	Calibrated age (yr B.P.)[c]	Source[d]
mc-1	Massada	200	23,690 ± 210	26,500	1
mc-2	Top of Ze'elim delta	300	13,300 ± 90	15,000	1
mc-3	Z7	290	45,000 ± 2,600	48,000	1
mc-4	Z7	284	33,200 ± 560	34,000	1
mc-5	Z7	279	24,400 ± 270	28,000	1
M2864	M1	333	16,167 ± 90	19,000	2
M2375	M1	338	23,320 ± 230	26,000	2
M2160	M1	342	30,150 ± 470	31,000	2
PZ1-3558	PZ1	268		18,500 ± 130	3
PZ1-3175	PZ1	263		24,700 ± 80	3
L21	PZ1	276		28,000 ± 580	3
L1	PZ1	301		56,000 ± 1360	3

Note. msl, mean sea level.

[a] mc-1 is an aragonite sample from the Massada cliff; for location of Z7 and M1, see Figure 6.; PZ1 is shown in Figure 2a.

[b] All samples are aragonite. Samples mc-1 to mc-5 were measured at the accelerator mass spectrometry Lab, University of Arizona.

[c] Samples mc-1 to mc-5 were calibrated according to Schramm *et al.* (2000), using reservoir effect of 1000 yr.

[d] Sources: 1, Bartov, 1999; 2, Schramm, 1997; 3, Schramm *et al.*, 2000 (U-Thages).

Cycle I is presented in the Massada plain only in sections Z1 and M1 as an offshore environment. The base of the cycle is defined by the unconformity between the Samra and the Lisan Formations. Since sections Z1 and M1 show mostly offshore facies, their height in the section represents the minimum lake-level elevation during cycle I. A better estimate is derived from the correlated lower part in PZ1, which is 70 m higher (Fig. 2b).

Cycle II (at the base of the upper sequence) begins with a sharp lake-level drop at ~48,000–43,000 cal yr B.P., whereas the top of the cycle is marked by a small-scale lake-level drop. Overall, this cycle is marked by a fining-upward sequence with frequent short-term erosional surfaces. At the lower boundary of cycle II a number of cross-bedded beach ridges are exposed. This boundary can be physically traced to the base of section Z6, where braided stream deposits are exposed.

Cycle III represents an example of a complete lateral transition from an alluvial to a deep-lake depositional environment, as shown in sections Z9 to Z1, respectively (Fig. 6). The lower boundary of this cycle is defined by an unconformity overlain by a flooding surface (e.g., elevation ~300 m below msl in section Z6). Section Z9 displays two coarsening-upward sequences. Eastward cycle III reveals fining of the sediment to coarse sand in section Z3, fine sand with climbing ripples and cross-beds in section Z2 (Fig. 4E), and offshore deposits in section Z1 (Fig. 4F).

Cycles IV and V in sections Z7 and Z8 become coarser to the north as a result of the proximity to the main input channel at the center of the Ze'elim fan-delta (see aerial photo in Fig. 6).

Cycle VI is mainly represented by the sequence boundary and occasional beach deposits of the Holocene regression.

In summary, the analysis of the sequence stratigraphy indicates several transgressive and regressive cycles in various time scales and dimensions. Cycle I is part of the high-stand systems tract cut by the unconformity at the base of cycle II. Cycles II–V represent a complete sequence from the low-stand transgressive phase that culminates at the high-stand systems tract of cycle V and then changes to a sharp regressive phase marked by the unconformity of cycle VI. These patterns are reflected in the detailed lake-level curve reconstructed below.

LAKE LEVELS OF LAKE LISAN

The lake-level history determined herein is based on our sequence stratigraphy interpretation, thermal ionization mass spectrometry U-series, and radiocarbon ages of the Lisan sections in the Perazim valley and the Massada plain (Fig. 7). The U-series and ^{14}C ages that were obtained for aragonite samples are used to anchor the relative chronology of the stratigraphic data to absolute ages (Fig. 6; Table 2). All dated samples are from aragonite laminae that bound beach deposits or other indicators of shallow-water environments (e.g., oscillatory rippled sand). Since the beach sediments were not dated directly, we have interpolated their age from the ages bounding the aragonite sequence (Table 2). In most cases, the calculated deposition rate is about 1 mm/yr, which is slightly higher than the rate estimated for the sequences of alternating aragonite and detrital laminae in the Perazim valley (about 0.8mm/yr; Schramm *et al.*, 2000). This higher sedimentation rate is related to the deposition of thicker fine-grained detrital laminae close to the fan-delta.

The transition from the Samra Formation to the Lisan Formation was dated at ~70,000 yr B.P. (Waldman *et al.*, 2000). The offshore facies that dominates the lower part of the section in the Perazim valley (dated at 70,000–55,000 cal yr B.P.) indicates that the lake level was above 306 m below msl. The first stratigraphic indication for lake-level lowering is at ~56,000 cal yr B.P. At

FIG. 6. The stratigraphic sections (Z1–Z9) in the southern Ze'elim fan-delta and Massada plain. Section locations are shown on the aerial photograph. Six cycles are marked on the sections. The base of cycle II is a sequence boundary representing a sharp lake-level drop between 48,000 and 43,000 cal yr B.P., whereas the top of the sequence is the base of cycle VI related to the lake-level drop in the Holocene. Each of the cycles represents a short period of lake-level oscillation as shown in Figure 7. Section M1 is located 1.5 km to the south of the area covered by the aerial photograph, and its top is at 330 m below msl. The dated samples are shown in sections M1 and Z7 (see Table 2).

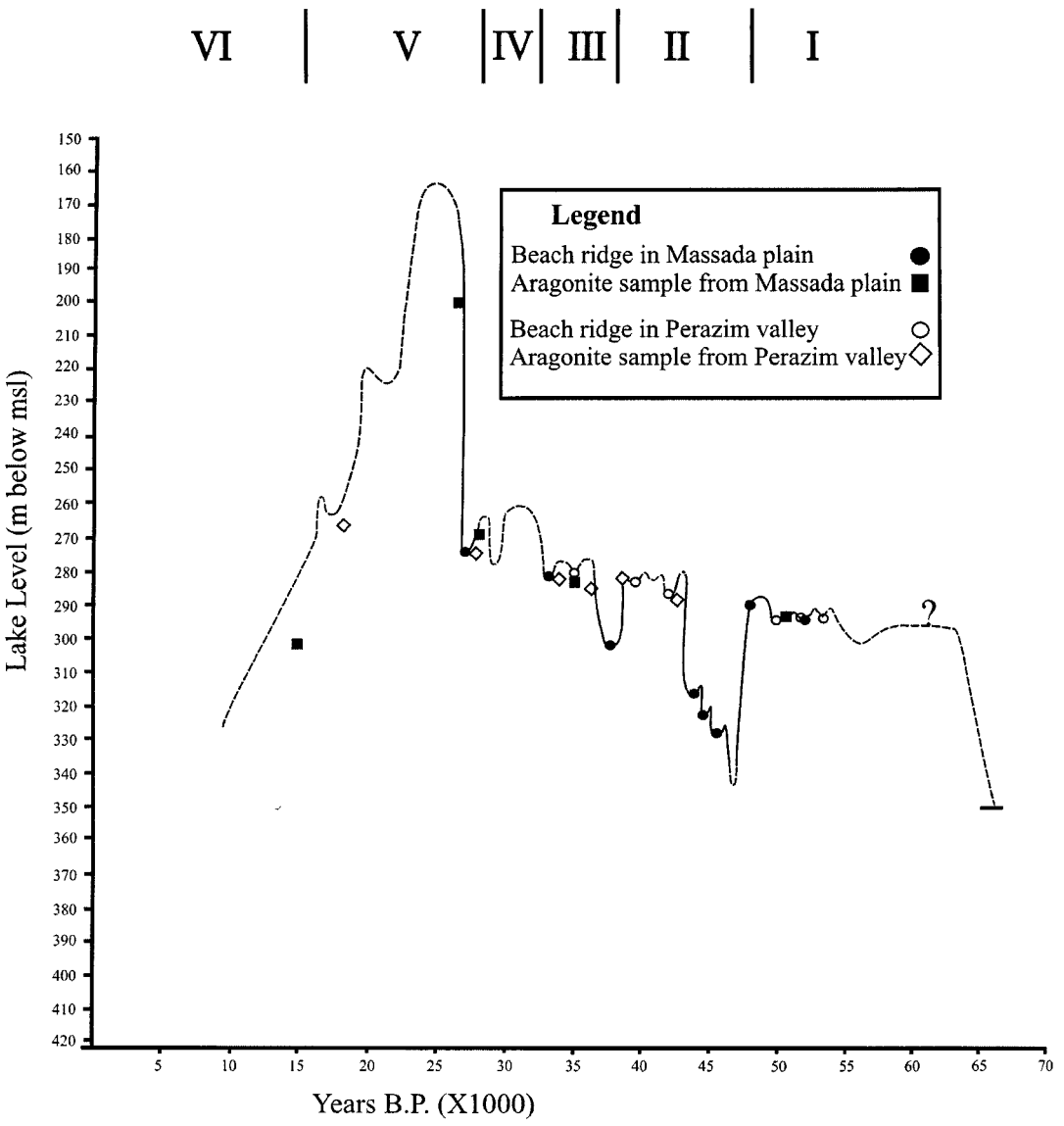

FIG. 7. Lake-level curve of Lake Lisan between 55,000–15,000 cal yr B.P. Open symbols-data from the Perazim valley (Machlus *et al.*, 2000) (PZ2); filled symbols-data from the Massada plain (Z1–Z11). Points on the curve represent beach ridges. Ages were interpolated from aragonite samples, assuming a 1-mm/yr deposition rate of laminated aragonite and the correlation shown in Figure 6. The chronology is based on ^{234}U-^{230}Th and ^{14}C ages of aragonite samples (Schramm *el al.*, 2000; Bartov, 1999; Table 2). The radiocarbon ages were calibrated to "calendar" years using the "Lisan calibration curve" and a 1000-yr-reservoir effect (Schramm *et al.*, 2000).

this time the lake level dropped and the lake overturned, according to Stein *et al.* (1997), as indicated by the precipitation of the three massive gypsum layers (Fig. 2). Above the gypsum layers, the sedimentation of aragonite and detrital laminae resumed, suggesting a rise in lake level. Our detailed analysis begins in the period postdating ~55,000 cal yr B.P. after the deposition of these gypsum layers.

55,000–48,000 cal yr B.P.

The lake level stabilized at an elevation between 297 and 291 m below msl, as recorded by shallow-water environments in the lower part of sections Z8, Z7, and PZ1 (Fig. 6). This segment represents the longest period of lake-level stabilization and is dominated by sedimentation of aragonite and detrital laminae.

48,000–43,000 cal yr B.P.

At ~48,000 cal yr B.P. the lake level dropped to ~340 m below msl. This drop is evident from an erosional channel with incipient soil on its banks that was observed in the PZ2 section, Perazim valley, at 289 m below msl (Machlus *et al.* 2000). In the Massada plain (M1 section, elevation 340 m below msl)

a widespread contemporaneous unconformity is exposed, and beach sediments were deposited laterally near the Ze'elim fandelta; these beach deposits probably mark the actual lake level at ~47,000 cal yr B.P., which is the lowest known level of Lake Lisan prior to its latest Pleistocene fall.

43,000–38,000 cal yr B.P.

The lake level rose by ~50 m and stabilized again between 280 and 290 m below msl. During this time interval, when the lake shores were located in the Perazim valley, as indicated by beach deposits in section PZ2, most of the Massada plain was about 40–50 m under water, and offshore lake sediments were deposited.

38,000–36,000 cal yr B.P.

At 38,000 cal yr B.P., the lake level dropped to ~300 m below msl. This regression is based on the identification of a shoreline in section Z6 (cycle III in Fig. 6) and is consistent with a basinward shift of facies. For this interval, the Perazim valley sections exhibit a clastic sequence.

36,000–33,000 cal yr B.P.

At 36,000 cal yr B.P. the lake level rose again to ~280 m below msl. This rise is marked by beach sediments that are exposed in both locations, the Perazim valley and the Massada plain, at high elevations of the Ze'elim fan-delta (sections Z7 and Z8 in Fig. 6).

33,000–27,000 cal yr B.P.

At 33,000 cal yr B.P. Lake Lisan levels rose from ~280 to ~265 m below msl (cycle IV in section Z8). Just before 27,000 cal yr B.P. the lake level dropped to 275 m below msl, as indicated by the beach deposits in section Z8 and shallow-water deposits in PZ1 in the Perazim valley.

27,000–15,000 cal yr B.P.

Starting at 27,000 cal yr B.P. the lake rose dramatically and approached its maximum elevation of >164 m below msl at ~25,000 cal yr B.P. The lake level fluctuated at a high elevation for ~2,000 years, then dropped again to ~270 m below msl at ~23,000–19,000 cal yr B.P. and to ~300 m below msl after 15,000 cal yr B.P. The low resolution of the lake-level curve during this period is due to the poor preservation of depositional indicators that onlap the escarpment. Our interpretation is mainly based on dated aragonite laminae from high elevations (sample mc-1 in Table 2) and on the onlap geometry of the basin margins. The lake-level drop is based on the preserved regressive beach lines from the high stand to the Holocene sediments and a dated sample from the top of the Ze'elim fan-delta at the elevation of 300 m below msl (sample mc-2 in Table 2). The small fluctuation at ~17,000 cal yr B.P. is represented by the two gypsum layers at the top of the sections in the Massada plain and the Perazim valley (Figs. 2 and 6). High-resolution data for that time span are currently being collected.

LAKE LEVELS, BASIN HYPSOMETRY, AND CLIMATE

Our analysis of Lake Lisan sediments indicates variations in the water level between 340 m and >164 m below msl during the period 55,000–15,000 cal yr B.P. (Fig. 7). For about half of this period, the lake displayed minor fluctuations within the interval of ~280–290 m below msl (see Fig. 7 for 55,000–48,000 cal yr B.P. and 42,000–30,000 cal yr B.P.). The modulations of the Lake Lisan level probably depended on two main parameters: (1) water input from the drainage basin and the lake levels in a terminal lake such as Lake Lisan, which are expected to be sensitive to climatic changes (Street-Perrott and Harrison, 1985; Stein *et al.*, 1997; Oviatt, 2000); and (2) physiographical features such as basin morphology and barriers between subbasins that could modify both the lake area and its volume at specific levels (e.g., Whol and Enzel, 1995).

The hypsometric diagrams of Lake Lisan show the curves of the lake surface area, the lake water volume (Fig. 8a), and the curve of incremental area change in km^2/m (Fig. 8b). These curves were generated from the Hall (1997) DTM database of 25 m × 25 m pixels and elevation resolution of 5 m. The incremental area curve reveals three peaks at elevations of 403, 385, and 240 m below msl that indicate relatively large changes in the lake area per unit depth. As an increase of the lake area increases the evaporation, it is expected that the lake level would be stable at the three peaks of area change. The hypsometric curve reveals that the peaks of 403 and 385 m below msl reflect the filling of the southern basin of the Dead Sea, which probably controlled the Dead Sea lake levels during the Holocene. The incremental area curve is essentially flat between the peaks of 385 and 240 m below msl (Fig. 8a); thus, the observed stable water level at ~280–290 m below msl is not predicted by the hypsometric curves. As for the reason for the stable level of ~280–290 m below msl, examination of the basin map and its topographic section (Fig. 1) reveals a sill at the Wadi Malih confluence, approximately at 280 m below msl. We suggest that this sill of Wadi Malih served as the controlling morphological feature that stabilized the Lake Lisan level at ~280–290 m below msl. Crossing this sill could not have been achieved without a dramatic increase in the total runoff to Lake Lisan. Therefore, we assume that the fast and intense lake rise from ~280 to ~240 m below msl at ~27,000 cal yr B.P. (Fig. 7) must have been associated with a significant climate change that provided a significant increase of flow to the lake.

The peak at 240 m below msl in the incremental area curve (Fig. 8b) reflects the added area of the Sea of Galilee. We do not regard this area as controlling Lake Lisan levels since it acted as a separate lake throughout Lake Lisan history except during the highest lake stand after 27,000 cal yr B.P.

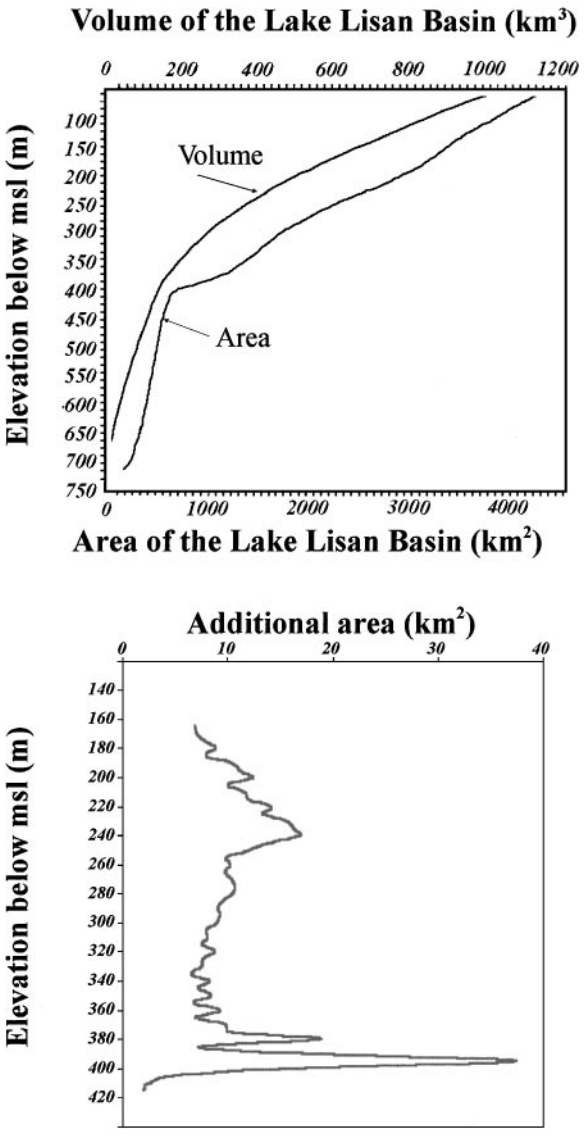

FIG. 8. (a) Hypsometric curves of the Dead Sea basin showing the surface area and volume of the water body that would be produced during a filling of Lake Lisan (after Hall, 1997). (b) A hypsometric curve showing the amount of the increased surface area (in km^2-per-meter elevation difference) as a function of the Lake Lisan water level. The small oscillations are probably noise caused by DTM with 25 m × 25 m surface elements.

CONCLUSIONS

1. The lake-level history of Lake Lisan was established by sequence stratigraphy analysis that provides information on transgressive and regressive phases of the lake and by correlation between dated sediments of shore and deeper water environments.

2. A complete stratigraphic sequence was identified between ~48,000 and 15,000 cal yr B.P. It commences with an erosional unconformity, continues with a lake-level rise that peaks at 25,000 cal yr B.P., and terminates with a sharp lake-level drop.

3. The lake-level reconstruction based on recognition of beach displays small fluctuations around 280–290 m below msl during most of the time interval of 55,000 and 30,000 cal yr B.P., punctuated by a sharp drop to ~340 m below msl at 48,000–43,000 cal yr B.P. At ~27,000 to 23,000 yr B.P. the lake rose to its maximum elevation of ~164 m below msl and then declined to ~300 m below msl at ~17,000 and 15,000 cal yr B.P.

4. The reconstructed lake-level curve reflects the physiography of the Dead Sea basin–Jordan Valley and the prevailing climatic conditions. Hypsometric considerations suggest that the critical elevations, where a large increase in lake size is expected, are at 403 and 385 m below msl. At these elevations the lake level is buffered. Lake Lisan was always higher than 380 m below msl, indicating a significantly large water contribution to the basin.

5. The long and repeated stabilization periods at 280–290 m below msl during Lake Lisan time indicate a combination between the hydrological control and the existence of a physical sill at this elevation. Crossing this sill could not have been achieved without a dramatic increase in the total water input to the lake, as occurred during the fast and intense lake rise from ~280 to 160 m below msl at ~27,000 cal yr B.P.

ACKNOWLEDGMENTS

We thank N. Waldman, O. Klein, and E. Stanislavsky for their help with the fieldwork; the Arab Potash Co. for their exceptional good will and assistance during the work at the Lisan Peninsula; J. K. Hall for the DTM data, Yossi Bartov, Z. B. Begin, H. Blatt, Z. Garfunkel, S. Goldstein, S. Marco, H. W. Posamentier, A. Sneh, T. Rockwell, and A. Starinsky for many helpful field discussions. Excellent reviews by J. Smoot and K. Adams improved the manuscript. This study was funded by the Israel Science Foundation (ISF, Grant 694/95). Additional funding was provided by and the German–Israel Foundation for research and development (GIF, Grant 546/97).

REFERENCES

Adams, K. D., and Wesnousky, S. G. (1998). Shoreline processes and age of the Lake Lahontan high-stand in the Jessup embayment, Nevada. *Geological Society of America* **110,** 1318–1332.

Bartov, Y. (1999). "The Geology of the Lisan Formation at the Massada Plain and the Lisan Peninsula." Unpublished M.Sc. thesis. The Hebrew University of Jerusalem [In Hebrew with an English abstract].

Begin, B. Z., Ehrlich, A., and Nathan, Y. (1974). Lake Lisan—The Pleistocene precursor of the Dead Sea. *Geological Survey of Israel Bulletin* 63.

Ben-David, H. (1998). "Modern and Holocene Debris Flows over the Western Escarpment of the Dead Sea." Unpublished M.Sc. thesis. The Hebrew University of Jerusalem [In Hebrew with extended English abstract].

Blair, T. C. (1999). Sedimentology of gravelly Lake Lahontan highstand shoreline deposits, Churchill Butte, Nevada, USA. *Sedimentary Geology* **123,** 199–218.

Bowman, D. (1997). Geomorphology of the Dead Sea western margins. *In* "The Dead Sea—The Lake and Its Setting." (T. M. Niemi, Z. Ben-Avraham, J. R. Gat, Eds.), pp. 217–225. Oxford Monographs on Geology and Geophysics No. 36.

Bowman, D., and Gross, T. (1992). The highest stand of Lake Lisan: ~150 meter below MSL. *Israel Journal of Earth Sciences* **41,** 233–237.

Enzel, Y., Kadan, G., and Eyal, Y. (2000). Holocene earthquakes inferred from a fan-delta sequence in the Dead Sea graben. *Quaternary Research* **53,** 34–48.

Ethridge, F. G., and Wescott, W. A. (1984). Tectonic setting, recognition and hydrocarbon reservoir potential of fan-delta deposits. *In* "Sedimentology of Gravels and Conglomerates" (E. H. Koster and R. J. Steel, Eds.), pp. 217–235. *Canadian Society of Petroleum Geologists, Memoir* No. 10.

Frostick, L. E., and Reid, J. (1989). Climatic versus tectonic control of fan sequences—Lessons from the Dead Sea, Israel. *Journal of the Geological Society of London* **146,** 527–538.

Garfunkel, Z. (1981). Internal structure of the Dead Sea leaky transform (rift) in relation to plate kinematics. *Tectonophysics* **80,** 81–108.

Hall, J. K. (1997). Topography and bathymetry of the Dead Sea Depression. *In* "The Dead Sea—The Lake and Its Setting" (T. M. Niemi, Z. Ben-Avraham, J. R. Gat, Eds.), pp. 11–21. Oxford Monographs on Geology and Geophysics No. 36.

Kadan, G. (1997). "Evidence for Dead Sea Lake-Level Fluctuations and Recent Tectonism from the Holocene Fan-Delta of Nahal Darga, Israel." Unpublished M.Sc. thesis, Ben-Gurion University of the Negev, Beer-Sheva.

Kaufman, A. 1971. U-series dating of Dead Sea Basin carbonates. *Geochimica et Cosmochimica Acta* **35,** 1269–1281.

Kaufman, A., Yechieli, Y., and Gardosh, M. (1992). Reevaluation of the lake sediment chronology in the Dead Sea basin, Israel, based on new $^{230}Th/^{234}U$ dates. *Quaternary Research* **38,** 292–304.

Ken-Tor, R., Agnon, A., Enzel, Y., Marco, S., Negendank, J., and Stein, M. (2001). High-resolution geological record of historical earthquakes in the Dead Sea basin. *Journal of Geophysical Research* **106,** 2221–2234.

Klein, C. (1984). Morphological evidence of lake-level changes, western shore of the Dead Sea. *Israel Journal of Earth Sciences* **31,** 67–94.

Machlus, M., Enzel, Y., Goldstein, S. L., Marco, S., and Stein, M. (2000). Reconstructing low-levels of Lake Lisan by correlating fan-delta and lacustrine deposits. *Quaternary International* **73/74,** 127–144.

Manspeizer, W. (1985). The Dead Sea Rift: Impact of climate and tectonism on Pleistocene and Holocene sedimentation. *In* "Strike-Slip Deformation, Basin Formation and Sedimentation" (K. T. Biddle and N. Christie-Blick, Eds.), pp. 143–158. *Society of Economic Petrology and Mineralogy* Special Publication No. 37.

Marco, S., and Agnon, A. (1995). Prehistoric earthquake deformations near Massada, Dead Sea graben. *Geology* **23,** 695–698.

Marco, S., Stein, M., Agnon, A., and Ron, H. (1996). Long-term earthquake clustering: A 50,000 year paleoseismic record in the Dead Sea graben. *Journal of Geophysical Research* **101,** 6179–6192.

Neev, D., and Emery, K. O. (1967). The Dead Sea; Depositional processes and environments of evaporites. *Israel Geological Survey Bulletin* 41.

Nemec, W., and Steel, R. J. (1984). Alluvial and coastal conglomerates: Their significant features and comments of gravelly mass-flow deposits. *In* "Sedimentology of Gravels and Conglomerates" (E. H. Koster and R. J. Steel, Eds.), pp. 1–31. *Canadian Society of Petroleum Geologists, Memoir* 10.

Nemec, W., and Steel, R. J. (1988). What is a fan-delta and how do we recognize it? *In* "Fan-Deltas: Sedimentology and Tectonic Settings" (W. Nemec and R. J. Steel, Eds.), pp. 3–13. Blackie, Glasgow/London.

Oviatt, C. G. (2000). Lacustrine features and global climate change. *In* "Quaternary Geochronology Methods and Applications" (J. S. Noller, J. M. Sowers, and W. R. Lettis, Eds.), pp. 470–478. Am. Geograph. Union, Washington, DC.

Posamentier, H. W., Allen, G. P., James, D. P., and Tesson M. (1992). Forced regression in a sequence stratigraphic framework: Concepts, examples and exploration significance. *Bulletin of American Association of Petroleum Geologists* **76,** 1687–1709.

Renaut, R. W., and Owen, R. B. (1991). Shore-zone sedimentation and facies in a closed rift lake: The Holocene beach deposits of Lake Bogoria, Kenya. *In* "Lacustrine Facies Analysis" (P. Anadon, L. I. Cabrera, and K. Kelts, Eds.), pp. 175–195. *International Association Sedimentologist Special Publication* 13.

Schramm, A. (1997). Uranium series and ^{14}C dating of Lake Lisan (Paleo-Dead Sea) sediments: Implications for ^{14}C time scale calibration and relation to global paleoclimate. Unpublished Ph.D. dissertation, Gottingen University, Germany.

Schramm, A., Stein, M., and Goldstein S. L. (2000). Calibration of ^{14}C time scale to >40 ka by ^{234}U-^{230}Th dating of Lake Lisan sediments (last glacial Dead Sea). *Earth and Planetary Science Letters* **175,** 27–40.

Sneh, A. (1979). Late Pleistocene fan-deltas along the Dead Sea Rift. *Journal of Sedimentary Petrology* **49,** 541–552.

Stein, M. (2000). The Late Pleistocene and Holocene sediments and tectonics of the Dead Sea Basin. *In* "Professional field trip guide book, The First Stephan Mueller Conference of the European Geophysical Society (EGS)" pp. 41–85.

Stein, M., Starinsky, A., Katz, A., Goldstein, S. L., Machlus, M., and Schramm, A. (1997). Sr-isotopic chemical and sedimentological evidence for the evolution of Lake Lisan and the Dead Sea. *Geochimica et Cosmochimica Acta* **61,** 3975–3992.

Street-Perrott, F. A., and Harrison, S. P. (1985). Lake-level and climate reconstruction. *In* "Paleoclimate Analysis and Modeling" (A. D. Hecht, Ed.), pp. 291–340. Wiley-Interscience, New York.

Waldman, N., Stein, M., Starinsky, A., and Katz, A. (2000). Limnological changes in Lake Samra from geochemical and mineralogical evidence of the sedimentary section of Peratzim Valley. Israel Geological Society Annual Meeting Abstracts, Ma'a lot, p. 126.

Wohl, E. E., and Enzel, Y. (1995). Data For Paleohydrology. *In* "Continental Paleohydrology" (K. J. Gregory, L. Starkel, and V. R. Baker, Eds.), pp. 23–59. Wiley, New York.